https://doi.org/10.1016/j.ast.2020.106327

Numerical analysis of the vibration-chemistry coupling effect on one-dimensional detonation stability

Ken Chun Kit Uy, Lisong Shi and Chih Yung Wen*

Department of Mechanical Engineering, The Hong Kong Polytechnic University, Kowloon, Hong Kong

E-mail for the *corresponding author: cywen@polyu.edu.hk

Abstract

A one-dimensional numerical simulation of detonation propagation is performed with an introduction of the vibrational relaxation mechanism in a single-step chemical model for the first time. This coupling mechanism is constructed based on the energy transfer between the translational-rotational mode and the vibrational mode, together with an averaged two-temperature model in chemical kinetics. A time ratio τ^{α} between the characteristic chemical time scale and the characteristic vibrational time scale is introduced to illustrate whether this coupling effect is crucial in stabilizing the detonation. The simulation is initialized first with an extended steady-state profile and the inclusion of the vibrational energy in the equations. For the particular case considered in this study with a nondimensional heat release $Q = 50$, a ratio of specific heat $\gamma = 1.2$, and a nondimensional characteristic vibrational temperature $\vartheta = 20$, the stability boundary is indicated at an activation energy $E_a = 26.47$ under thermal equilibrium. Two mildly unstable cases for a Chapman-Jouguet (CJ) detonation and an overdriven detonation are then studied with the variation of τ^{α}. The results reveal that the detonation is stabilized by the vibrational nonequilibrium effect with a smaller pulsation amplitude and a longer oscillation period in the shock pressure history, and the neutral stability is shifted. For the CJ detonation case, the critical τ^{α} below which the coupling effect is significant is 7.2. The stabilization of detonation can be attributed to the change of overall chemical reaction rate and thus a shift of the stability limit towards higher activation energy. For an overdriven detonation, the critical τ^{α} is approximately 21 for the studied cases. Since the changes in both overdriven factors f and τ^{α} contributed to the stabilization of detonation, a reduction of the neutral stability limit of f is foreseen when the coupling effect is significant. Lastly, the effect of different ϑ on the stability limit is demonstrated at

equilibrium state with vibrational energy included and it is suggested that the shift of stability limit would reach the maximum at around $\vartheta = 15$. This inaugural work provides a reference on the importance of considering thermal nonequilibrium flow in detonation stability and the implication to the related engine design.

Keywords: detonation; stability; vibrational nonequilibrium; numerical simulation

1. Introduction

Detonation occurs when a supersonic wave induces shock compression, heats up the reactants in the flow and initiates chemical reactions, such that the energy released in the form of heat sustains propagation. Although the establishment of a self-sustained detonation under a short flow-through time scale in the detonation engine design remains a challenge, the great thermal propulsion performance of the detonation engine still attracts researchers' attention nowadays. Many efforts have been done in numerical simulations to study the detonation engine performance under practical operation states, for instance, the pulse detonation engine (PDE), rotating detonation engine (RDE) and oblique detonation wave engine (ODWE) [1-3]. In particular, as pointed out in the literature, the role that the detonation stability plays in supersonic propulsion devices is worth to be investigated theoretically, experimentally and numerically [4].

A detonation wave structure can be studied one-dimensionally by a well-known steady-state solution named the Zel'dovich–von Neumann–Döring (ZND) model developed in the 1940s [5-7]. Nevertheless, a gaseous detonation wave in reality often exists in multidimensional form and is inherently unstable due to the interaction between the transverse wave and the leading shock at the triple point within the reaction zone. A cell or a diamond pattern of cellular instability can thus be observed in a two-dimensional rectangular channel when the detonation wave propagates [8]. However, to some extent, detonation can be one dimensional in nature, and thus, the corresponding pulsating detonation stability has been studied extensively in past decades [9-11].

To investigate the instability of a detonation wave from an analytical approach (for instance, the linear stability analysis), it is common to solve the steady one-dimensional conservation equations first with a single, irreversible reaction in an Arrhenius form and then introduce small perturbations in the solution to see if the

amplitudes of the perturbations grow or decay. The use of an idealized chemical model enables investigators to check the reliability of the cases before conducting numerical simulations with detailed chemistry involving multiple species. In the middle of the 20th century, Erpenbeck [12-14] conducted an extensive mathematical study on this idealized one-reaction detonation instability using an initial value Laplace transform approach. Thereafter, Lee and Stewart [15] revisited the problem by introducing a normal mode approach in linear stability analysis. While fundamental detonation physics has been assessed with this stability analysis, the increase in computational power in recent years has enabled a series of parametric studies regarding the dependence on activation energy, overdriven factors, heat release, etc with this simplified chemical model. The fairly accurate prediction of the stability boundaries and the oscillation periods in slightly unstable pulsating detonation by linear stability analysis helps in establishing a more realistic simulation involving complicated chemical reactions. By contrast, in the analysis on shock pressure history from numerical simulation, the governing equations are solved without introducing small perturbation particularly. The startup errors are sufficient to trigger the pulsating instability. However, the computational cost heavily depends on the grid resolution, particular near the stability boundary where the growth or decay rate of the profile is small. Examples of such scenarios have been discussed numerically and analytically by different authors in recent decades [16-19].

On the other hand, recent studies have revealed that the mechanism of vibrational relaxation is crucial in the delay of flame ignition and stabilization of supersonic scramjet combustion [20-22] and in gaseous detonation to account for the differences in cell sizes between experiments and simulations [23-25]. From statistical thermodynamic, molecules are known to consist of translational, rotational, vibrational, and electronic energy modes [26]. After encountering the shock, translational equilibrium can be established quickly in less than 10 molecular collisions, while the rotational equilibrium can be obtained within 20 molecular collisions. However, thousands of collisions are required for the vibrational mode to establish its equilibrium, and therefore is notably important in this study [27]. For instance, the ignition time scale and the vibrational time scale of a typical H_2/air detonation were investigated by Taylor et al. [25], and they revealed that the ignition time scale can be less than the vibrational time scale. In this context, Shi et al. [23] simulated both one-dimensional (1D) and two-dimensional (2D) H_2/O_2 detonation with 70% argon dilution and reported that the case under vibrational nonequilibrium shows significant elongation in the half-reaction length and an enlarged

detonation cell size. The computed cell size becomes comparable with the experimental size, and the significant influence of the vibrational relaxation mechanism is therefore demonstrated. To further expand the theoretical understanding of the coupling effect between vibrational relaxation and chemical reaction on the half reaction length and the cell size, Uy et al. [24] proposed an extended ZND model with a simplified vibration-chemistry coupling mechanism. It is shown that the energy transfer between the translational-rotational mode and the vibrational mode reduces the effective temperature and slows down the chemical reaction rate, which is manifested in terms of elongation in the half-reaction length within the reaction zone. A critical time ratio of the chemical time scale versus the vibrational time scale, below which the vibrational nonequilibrium should be considered, was reported in the related parametric studies.

Although the effect of the coupling mechanism between the chemical reactions and molecular vibrational nonequilibrium has been reported by many authors, the consideration of this coupling mechanism in detonation stability analysis has not been studied before. Based on the findings of stability analyses with different chemical kinetics in previous papers, a shift of the neutral stability limit is expected for detonation in a state of vibrational nonequilibrium compared with that in a state of equilibrium.

In this paper, a single-step chemical reaction in an Arrhenius form coupled with a vibrational relaxation mechanism is considered in a detonation stability analysis through numerical simulation. The time ratio introduced by Uy et al. [24] is adopted to denote the different states of thermal nonequilibrium in the detonation. The present study aims to numerically investigate the possibility of a shift in the neutral stability range for the selected unstable cases under different time ratios. Through this study, a critical time ratio for which the solution converges to a state of equilibrium is also suggested.

2. Mathematical model

2.1 Governing equations

To simulate the detonation propagation inside a channel, one-dimensional reaction Euler equations are applied, and the corresponding normalized form is presented as follows:

$$\frac{\partial \rho}{\partial t} + \frac{\partial (\rho u)}{\partial x} = 0 \tag{1}$$

$$\frac{\partial(\rho u)}{\partial t}+\frac{\partial(\rho u^2+p)}{\partial x}=0 \tag{2}$$

$$\frac{\partial(\rho e)}{\partial t}+\frac{\partial[u(\rho e+p)]}{\partial x}=0 \tag{3}$$

Referring to previous works [23, 24, 28], under a state of vibrational nonequilibrium, the energy equation is reformulated such that vibrational energy and translational-rotational energy terms are separated for investigation. Thus, the specific internal energy e, specific translational-rotational energy e_{tr}, and specific vibrational energy e_{v} are described as follow, while ignoring the electronic mode:

$$e=e_{\mathrm{tr}}+e_{\mathrm{v}}+\frac{u^2}{2}-\lambda Q \tag{4}$$

$$e_{\mathrm{tr}}=\frac{\epsilon}{2}T_{\mathrm{tr}},\epsilon=\frac{2}{(\gamma-1)} \tag{5}$$

$$e_{\mathrm{v}}=\frac{\vartheta}{\exp(\vartheta/T_{\mathrm{v}})-1} \tag{6}$$

where ρ, u, p, Q, γ, ϵ, ϑ, T_{tr}, T_{v} and λ are the density, velocity, pressure, local heat release, the ratio of specific heats, degree of freedom of reactant (or product) molecules, characteristic vibrational temperature, translational-rotational temperature, vibrational temperature and the reaction progress variable for the product, respectively. λ is equal to zero at the upstream state and is equal to 1 at the downstream state, representing the completion of the reaction. Notably, Eqs. (5) and (6) are in nondimensional forms so that the gas constant R is not seen. The determination of these two energy modes follows the approach from statistical thermodynamics [26]. T_{v} can be obtained through Newton's iteration with the known function e_{v} expressed in Eq. (6).

For the chemical kinetics, a simplified single-step Arrhenius model is applied to describe the chemical reaction process. Park's two-temperature model is adopted to represent the coupling of the translation-rotational mode with the vibrational mode. Park's two-temperature model has been demonstrated in many works related to high-temperature flow, particularly in understanding the fundamental physics of detonation and hypervelocity flows due to its simplicity. The expressions of the chemical kinetics with Park's two-temperature model are given as:

$$\frac{\partial(\rho\lambda)}{\partial t}+\frac{\partial(\rho u\lambda)}{\partial x}=\rho k(1-\lambda)\exp\left(-\frac{E_a}{T_{avg}}\right) \tag{7}$$

$$T_{avg}=\sqrt{T_{\mathrm{tr}}T_{\mathrm{v}}} \tag{8}$$

where k and E_a denote the chemical rate constant and activation energy, respectively. k is evaluated with different choices of E_a such that the half-reaction length computed is fixed (in this case, is equal to unity) at the thermal equilibrium condition [29].

To manifest the importance of the vibrational relaxation mechanism in the simulation, the Landau-Teller model is adopted to describe the energy exchange between the translational-rotational mode and the vibrational mode. The transfer rate equation is then formulated as:

$$\frac{\partial(\rho e_{\mathrm{v}})}{\partial t}+\frac{\partial(\rho u e_{\mathrm{v}})}{\partial x}=\rho\frac{e_{\mathrm{v}}^{eq}-e_{\mathrm{v}}}{\tau_{\mathrm{v}}} \tag{9}$$

where e_{v}^{eq} and τ_{v} are the vibrational energy at the thermal equilibrium state and the vibrational relaxation time scale, respectively. By assuming that the translational-rotational mode and the vibrational mode reach the equilibrium state immediately after the shock, e_{v}^{eq} described in Eq. (6) is a function of the translational-rotational temperature T_{tr} (in other words, $T_{\mathrm{v}}=T_{\mathrm{tr}}$). Unlike the single-step Arrhenius rate, which depends on the chemical rate constant k, the vibrational energy change rate in Eq. (9) depends on the vibrational relaxation time scale τ_{v}.

For the thermal equilibrium case with the consideration of the vibrational energy term inside the energy equation, i.e., Eq. (4), the relaxation rate equation is neglected in the simulation, as the vibrational equilibrium is assumed to be quickly established immediately behind the shock. In this case, $T_{\mathrm{tr}}=T_{\mathrm{v}}$ is held within the reaction zone.

Note that the parameters presented in this paper are nondimensionalized with respect to the corresponding values at the initial reactant state, which is denoted with the subscript 0: (the superscript * represents the dimensional quantities)

$$\rho=\frac{\rho^*}{\rho_0},p=\frac{p^*}{p_0},T=\frac{T^*}{T_0},u=\frac{u^*}{\sqrt{RT_0}},x=\frac{x^*}{\mathcal{L}_{1/2}},\vartheta=\frac{\vartheta^*}{T_0},$$
$$t=\frac{t^*}{\mathcal{L}_{1/2}/\sqrt{RT_0}},Q=\frac{Q^*}{RT_0},k=\frac{k^*}{\sqrt{RT_0}/\mathcal{L}_{1/2}},E_a=\frac{E_a^*}{RT_0} \tag{10}$$

where $\mathcal{L}_{1/2}$ is the half-reaction length and is defined as the distance from the shock to where one half of the reactant is consumed. It is set as unity in this study.

2.2 Evaluation of vibrational relaxation time scale

One of the motivations in this study is to determine whether the detonation phenomena would be stabilized by the thermal nonequilibrium effect. As discussed in the previous section, the different vibrational time scales will alter the rate of change of vibrational energy in the vibrational relaxation process. Therefore, a time ratio of the chemical time scale to the vibrational time scale τ^{α} is introduced based on our previous analyses [24, 28] to characterize the shift of the equilibrium state:

$$\tau^{\alpha} \equiv \frac{\tau_c}{\tau_{\mathrm{v}}} \tag{11}$$

where τ_c is the chemical time scale evaluated from the single-step Arrhenius rate and is defined as the time for which one-half of the reactant is consumed. τ_c is a fixed parameter if the corresponding parameters in the chemical model are fixed. Therefore, the evaluation of τ_{v} to indicate different degrees of vibrational nonequilibrium becomes possible based on the input of different time ratios τ^{α}. Notably, the vibrational relaxation time in the realistic detonation simulation varies within the reaction zone if an empirical model is implemented (commonly the Millikan and White model for gaseous mixture [30]). Uy et al. [28] has presented a detailed procedure to tune the model of vibrational relaxation time for replicating a realistic reactive mixture in their study on the prediction of half reaction length in $H_2/O_2/Ar$ detonation. However, the complex mechanism involving multiple species collisions complicates the analysis. Therefore, τ^{α} is utilized instead for the parametric study of the effect of vibrational nonequilibrium here.

2.3 Establishment of steady-state profile

For all cases of detonation instability, a steady-state profile is required as the initial study condition. The necessity of considering detonation instability from a steady, planar state was discussed in the previous study by Sharpe and Falle [9]. To include the change in the vibrational energy term based on the formulation in Eq. (4), the Rankine-Hugoniot relation is rewritten accordingly, and the new steady-state ZND solution is expressed as follows (subject to the specific volume v and pressure p across the shock profile):

$$v = \frac{\gamma M^2 + 1}{M^2(\gamma + 1)}[1 \mp w\xi(\lambda, e_{\mathrm{v}})],$$
$$p = \frac{\gamma M^2 + 1}{\gamma + 1}[1 \pm \gamma w\xi(\lambda, e_{\mathrm{v}})]$$

$$\xi(\lambda, e_{\mathrm{v}}) = \sqrt{1 + \frac{e_{\mathrm{v}} - \lambda q}{\Omega}}, \Omega = \frac{\gamma(M^2-1)^2}{2M^2(\gamma^2-1)}, w = \frac{M^2-1}{\gamma M^2+1} \tag{12}$$

where M is the Mach number. Note that the terms λ and e_{v} within the reaction zone can be evaluated by both the single-step Arrhenius equation and the Landau-Teller model, i.e., Eqs. (7)-(9). To describe an overdriven detonation, a degree of overdrive f is defined based on the relation between the steady detonation speed D and the Chapman-Jouguet detonation speed D_{CJ} (and hence the Mach number), which is expressed below:

$$f = \left(\frac{M}{M_{CJ}}\right)^2 \tag{13}$$

3. Computation method

In this paper, the unsteady Euler equations coupled with chemical and vibrational mechanisms are solved numerically by the conservation element and solution element (CE/SE) method with second-order accuracy [31]. This numerical method unifies the treatment of both space and time and has been applied in many studies related to hypersonic flows [32-36] and gaseous detonation [23, 36].

The computations are initially set up based on the steady-state solution presented in section 2.3. According to previous research on detonation stability by Sharpe and Falle [9], an effective numerical grid resolution of 128 points per half-reaction zone length (128 p/ $\mathcal{L}_{1/2}$) was suggested for numerical convergence and to resolve the detailed structures of the pulsating detonation. Note that the simulated detonation wave propagates from left to right in the positive *x*-direction. As discussed by Sharpe and Falle [9], to avoid the boundary effect during the calculation, a zero gradient boundary condition was initially set at the left-hand side with a half-reaction length at least 1000 behind the position of the shock.

Before the instability analysis, a one-dimensional piston-supported detonation case with $E_a = 50$, $Q = 50$, $\gamma = 1.2$ and $f = 1.6$ reported by Shen and Parsani [37] was simulated for code validation. The average periods of oscillation computed by our code for the cases with the grid resolutions of 10 points per $\mathcal{L}_{1/2}$ (p/ $\mathcal{L}_{1/2}$), 20 p/ $\mathcal{L}_{1/2}$, 40 p/ $\mathcal{L}_{1/2}$ and 80 p/ $\mathcal{L}_{1/2}$ are 7.60, 7.43, 7.37 and 7.34, respectively. The percentage differences with the same cases computed in [37] are within 0.01%. The code is well validated.

4. Results and Discussion

In this study, $\gamma = 1.2$, $Q = 50$ and $\vartheta = 20$ are fixed to illustrate the importance of vibrational nonequilibrium in the 1D detonation simulation. The stability boundary for the equilibrium state with vibrational energy included is determined first, and two mildly unstable cases for a CJ detonation and an overdriven detonation are then studied by varying the time ratio τ^{α}. Notably, the choice of ϑ depends on the range of normalized vibrational temperature that is interested in the problem and is arbitrarily fixed here for easy demonstration in Sections 4.1, 4.2 and 4.3. The effect of different ϑ on the shift of stability boundary for detonation at equilibrium state with vibrational energy included is studied in Section 4.4.

4.1 Stability boundary study for equilibrium state with vibrational energy included

The shock pressure history for the thermal equilibrium case with vibrational energy included is first investigated to represent the development of detonation instability. By varying the activation energy E_a at fixed parameters of the heat release Q and the specific heat ratio γ in the chemical kinetics, the neutral stability limit below which the detonation becomes stable is identified. As the detonation wave propagates, the detonation is determined to be unstable if the recorded shock pressure grows with time, while the detonation is considered stable if the shock pressure decays with time. For instance, the pressure histories of the detonation specified at $Q = 50$ and $\gamma = 1.2$ with different E_a values are presented in Fig. 1. For the case of E_a at 26.30 (Fig. 1a), the perturbation of the propagating detonation decays with time, denoting that a stable condition would eventually be reached. In contrast, a growing perturbation is observed as time goes on in the case of E_a at 26.70 (Fig. 1b). These results reveal that the neutral stability boundary will fall between these two values, and it is found that the limit reaches approximately $E_a = 26.47$, i.e., above which the detonation is unstable. Compared with the neutral stability limit of $E_a = 25.27$ found by Sharpe and Falle [9] under thermal equilibrium for the same Q and γ but without consideration of the vibrational energy, the introduction of the vibrational energy term in Eq. (4) raises the stability boundary with the conventional ZND solution, indicating that the presence of vibration energy will lead

to the detonation stability.

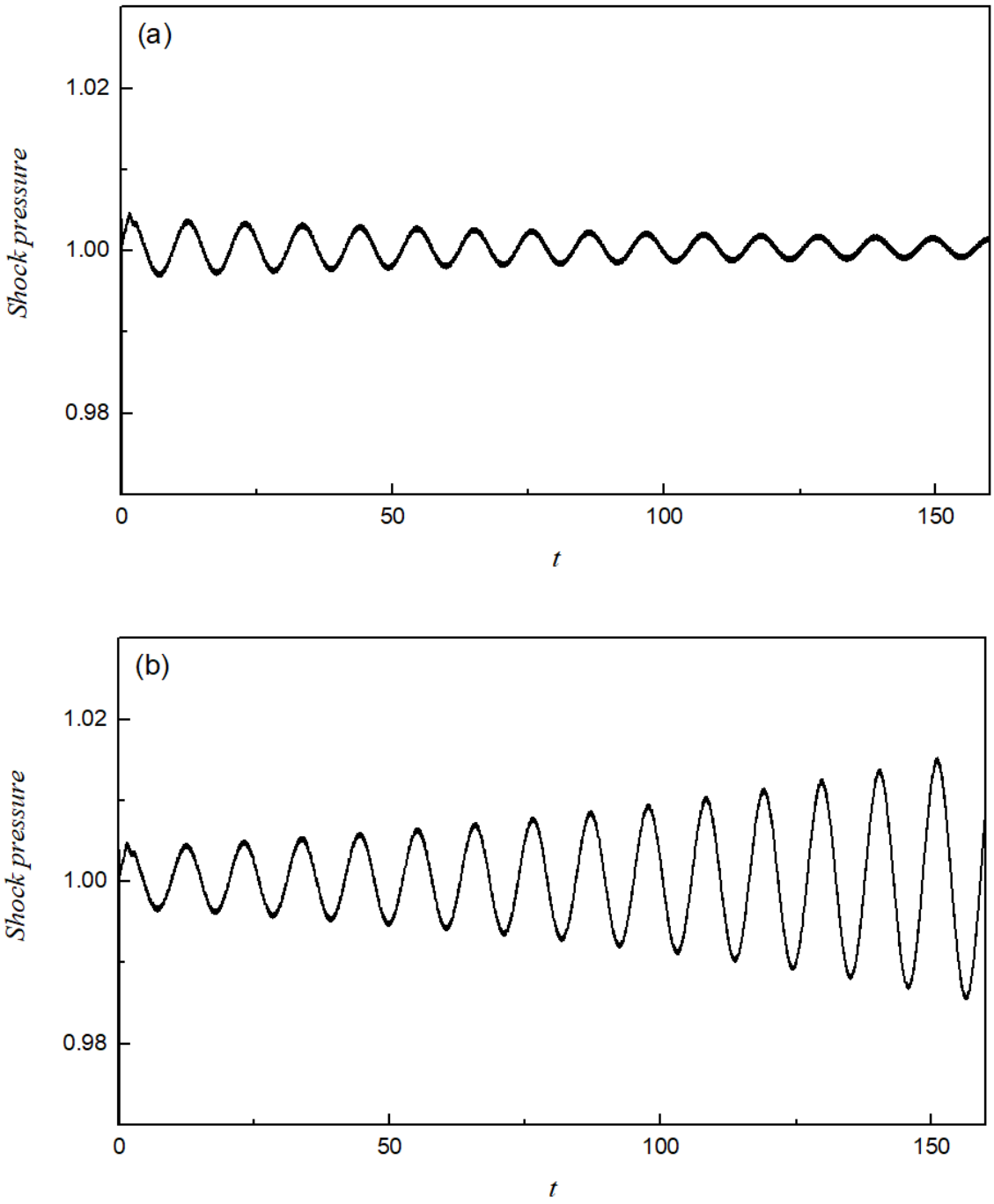

Fig. 1. Shock pressure history at a) $E_a = 26.30$ and b) $E_a = 26.70$ under the vibrational equilibrium (*eq*) assumption. Other fixed parameters are $Q = 50$, $\gamma = 1.2$, $\vartheta = 20$ and $f = 1.0$

Furthermore, a grid convergence study is conducted and is presented in Table 1, showing the determination of the neutral stability boundary under different numerical resolutions. The result confirms that a resolution of 128 grids per half-reaction length of

the steady-state ZND detonation is sufficient to provide a converged value of the limit, thus proving the statement mentioned in section 3.

Table 1

Determination of neutral stability boundary for different numerical resolutions

Grids per half-reaction length	E_a
8	26.36
16	26.38
32	26.44
64	26.46
128	26.47
256	26.47

4.2 Shock pressure history of a mildly unstable CJ detonation with different τ^α

It is known that the increase in activation energy E_a in detonation simulation always leads to an increase in instability. To investigate whether the propagating detonation would be stabilized or destabilized at different states of vibrational nonequilibrium, a variation of τ^α is tested in the case of $E_a = 27$, which is unstable if at thermal equilibrium. Fig. 2 shows the shock pressure histories for τ^α at 3, 5, 7, 9 and 11 with the equilibrium case as the benchmark solution. Generally, the peak amplitude is smaller in cases with lower τ^α, and the period of oscillation becomes longer as τ^α decreases. For instance, the period of oscillation at $\tau^\alpha = 3$ is 12.89 on average, whereas that of the equilibrium case is 10.66. Fig. 3 shows the temporal variations in the peak pressure difference for the corresponding profiles in Fig. 1, and the difference is calculated by subtracting each peak pressure from the 1st peak value in the shock pressure histories accordingly. In other words, the 1st peak amplitude serves as a reference to determine whether the perturbation of the propagating detonation grows or decays with time.

From Fig. 3, the peak amplitudes decay with time in the case of $\tau^\alpha = 3, 5$ and 7 and the decay rate becomes faster at a smaller τ^α. These observations deviate from the

expectation of growing perturbations at $E_a = 27$ under thermal equilibrium. Instead, both the decaying pulsation and the longer period of oscillation indicate that the propagation detonation is stabilized because of vibrational nonequilibrium. As τ^α decreases (recall the definition of $\tau^\alpha \equiv \tau_c/\tau_\mathrm{v}$ in Eq. (11)), the chemical time scale τ_c and the vibrational time scale τ_v become comparable with each other and the condition becomes more thermal nonequilibrium. At $\tau^\alpha > 9$, the pulsation increases as time proceeds, which implies that the detonation becomes unstable as it approaches thermal (vibrational) equilibrium, i.e., $\tau_c \gg \tau_\mathrm{v}$. After several computations within the selected τ^α range, the critical τ^α for which the detonation is stabilized at $E_a = 27$ is 7.2. The stabilization in detonation under the vibrational nonequilibrium state is due to the presence of the exchange of energy between the translational-rotational mode and the vibrational mode within the chemical reaction. Although no further conclusion could be made on the relation between the overall reaction rate and the detonation stability, it is clear that the latter one is sensitive to the vibrational relaxation process. This finding is analogous with the case of the change of half reaction length in detonation considering vibrational nonequilibrium, as reported by Uy et al [24], in which the computed half-reaction length increases as τ^α decreases. Shi et al [23] also share a similar conclusion on the fact that time is needed before the onset of severe chemical reaction, and thus leads to the elongated half-reaction length computed at the vibrational nonequilibrium in the numerical simulation using detail chemistry. Following the above discussion, a shift of the neutral stability limit of the activation energy to a higher value is foreseen if the vibrational nonequilibrium effect plays a significant role in chemical kinetics.

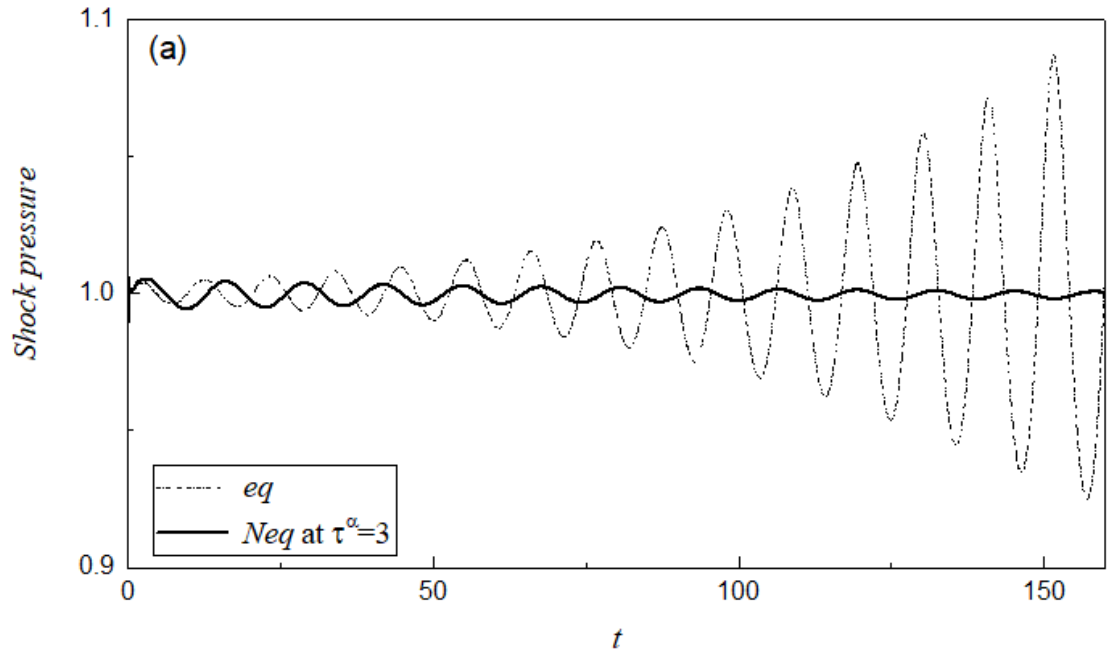
(a)
1.1
1.0
0.9
Shock pressure
0
50
100
150
t
eq
Neq at τ^α=3

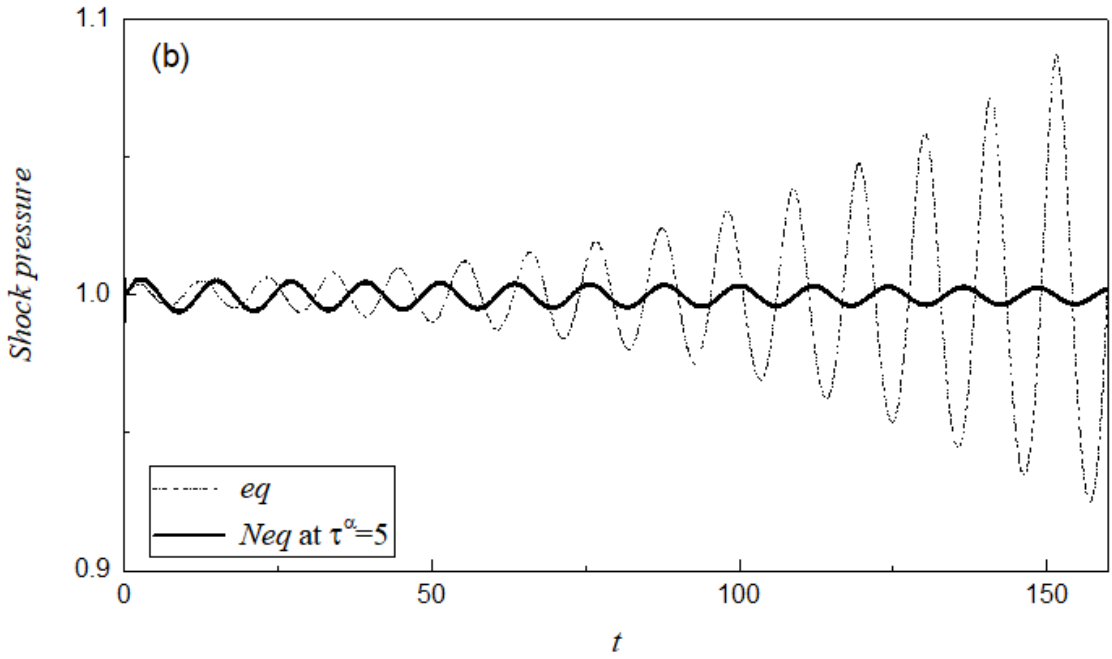
(b)
1.1
1.0
0.9
Shock pressure
0
50
100
150
t
eq
Neq at τ^α=5

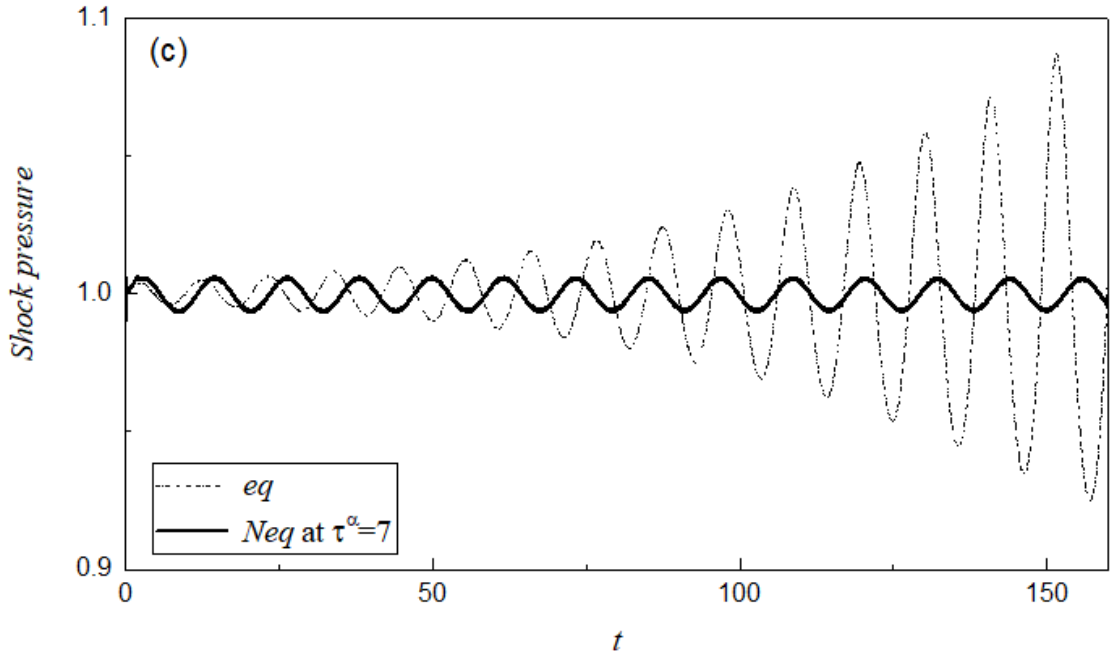
(c)
1.1
1.0
0.9
Shock pressure
0
50
100
150
t
eq
Neq at τ^α=7

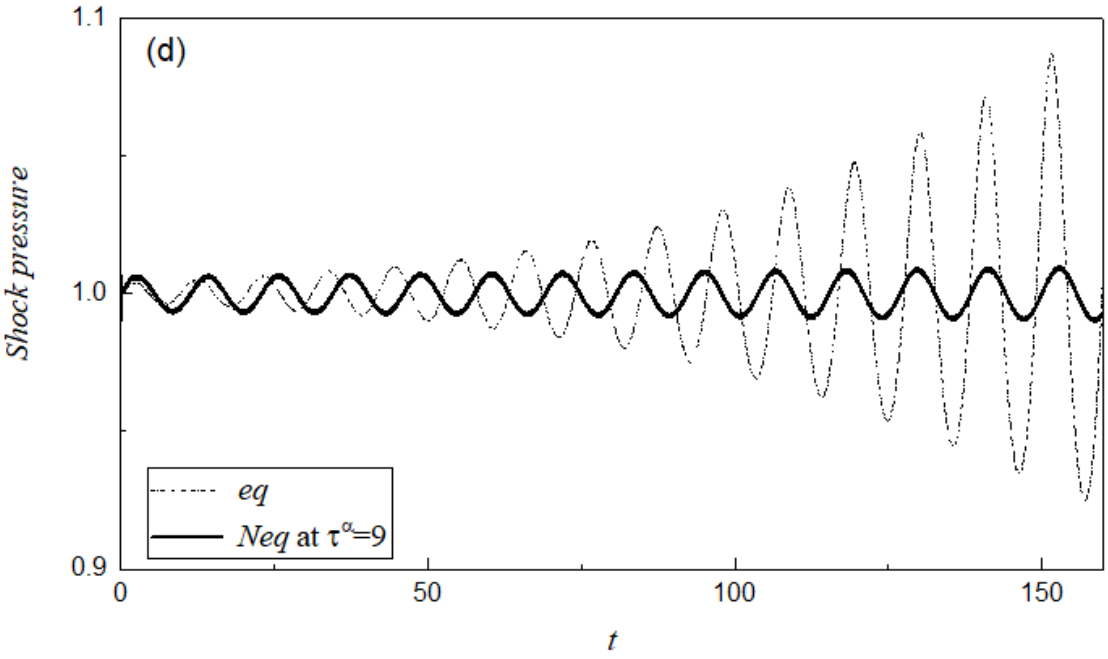
(d)
1.1
1.0
0.9
Shock pressure
0
50
100
150
t
eq
Neq at τ^α=9

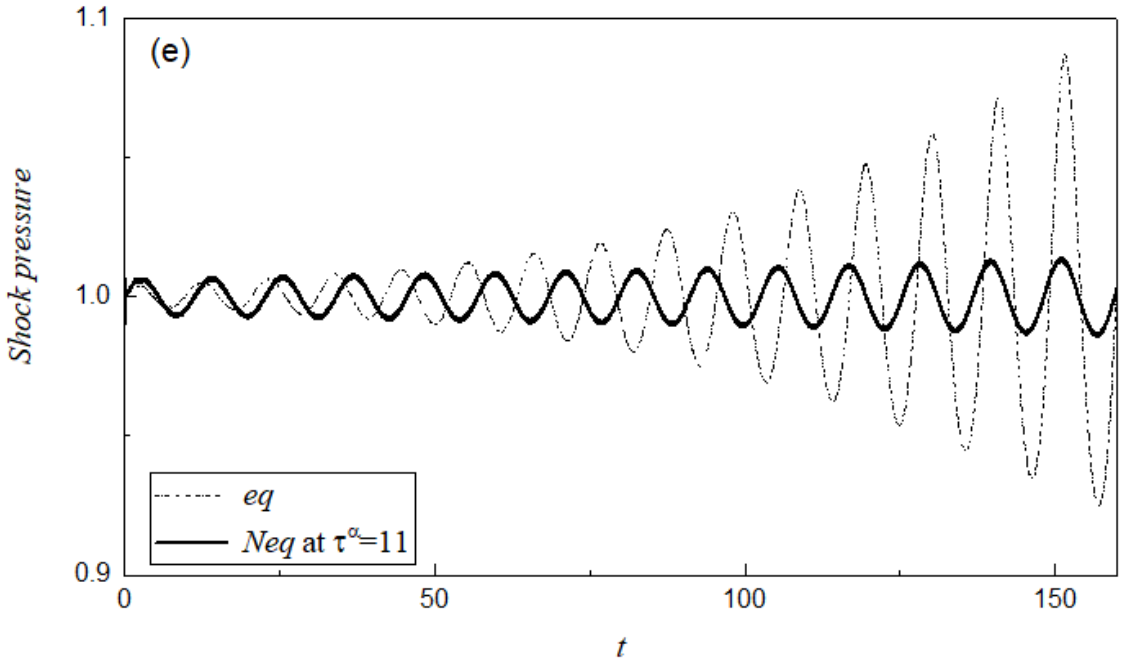

Fig. 2. Shock pressure history at $E_a = 27$ for vibrational nonequilibrium (*Neq*) cases at a) $\tau^{\alpha} = 3$ (period = 12.89) b) $\tau^{\alpha} = 5$ (period = 12.10) c) $\tau^{\alpha} = 7$ (period = 11.75) d) $\tau^{\alpha} = 9$ (period = 11.51) and e) $\tau^{\alpha} = 11$ (period = 11.39) with the equilibrium case (*eq*) (period = 10.66) as reference. Other fixed parameters are $Q = 50$, $\gamma = 1.2$, $\vartheta = 20$ and $f = 1.0$.

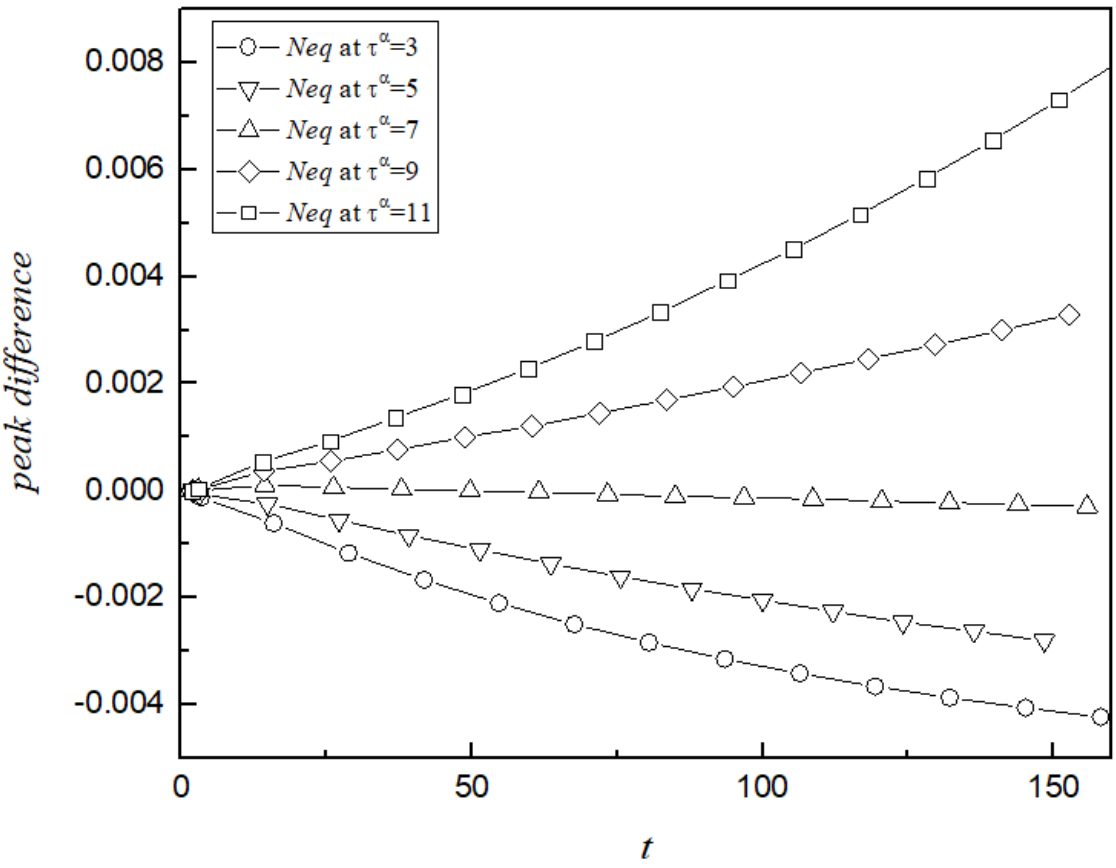

Fig. 3. The variations in the peak pressure difference with time for different vibrational nonequilibrium (*Neq*) cases in Fig. 2 at $\tau^{\alpha} = 3, 5, 7, 9$ and 11.

4.3 Shock pressure history of a mildly unstable overdriven detonation with different τ^{α}

Another factor that would stabilize or destabilize the detonation propagation is the detonation speed attributed to the overdriven factor f. Generally, the increase in f in the numerical simulation of detonation can stabilize the pulsation as the detonation wave propagates. In linear stability analysis, it is common to study the behaviour of an overdriven detonation over a CJ detonation [15, 38] because detonation, in reality, can be propagated in a piston-supported form [39]. Moreover, different modes of detonation propagation can be illustrated through variations in f [40]. For a case of detonation at $E_a = 50$, $Q = 50$ and $\gamma = 1.2$ without considering the presence of vibrational energy, the stability limit above which the detonation is stable is $f = 1.731$ [15]. Therefore, in this study, an unstable case with $f = 1.6$ is investigated while other parameters in the simulation, i.e., values of E_a, Q and γ, are fixed accordingly as mentioned above.

Different τ^{α} denoting the state of vibrational nonequilibrium by means of the time scale ratio are allowed to vary in the computation. Fig. 4 shows the shock pressure history with $\tau^{\alpha} = 5,\ 10,\ 20$ and 30. A peak difference analysis similar to that in section 4.2 is performed and is presented in Fig. 5. Noted that the initial drops of peak pressure difference in Fig. 4 and Fig. 5 are due to the numerical startup errors, and a stable configuration of the profile would be obtained eventually [16].

Under the fixed f, the propagating detonation is stabilized under the small τ^{α} value, which shows the same effect as that in section 4.2. A longer period of oscillation is again observed as τ^{α} decreases, where the increase of period oscillation can reach 15% (at $\tau^{\alpha} = 5$) compared with that in the equilibrium cases. From the peak difference analysis, the critical τ^{α} below which the vibrational relaxation mechanism is significant is approximately 21, where the pulsation shows a decay with time. These results indicate that the neutral stability limit of the overdriven factor f can be shifted to a smaller value as τ^{α} decreases. Since both the increase of f (considering detonation speed) and the decrease of τ^{α} (considering vibrational-chemical coupling effect) contribute to the stabilization in detonation analyses, with the decrease of τ^{α} indicating the significant role of vibrational relaxation in chemical kinetics, the neutral stability of f is reduced accordingly.

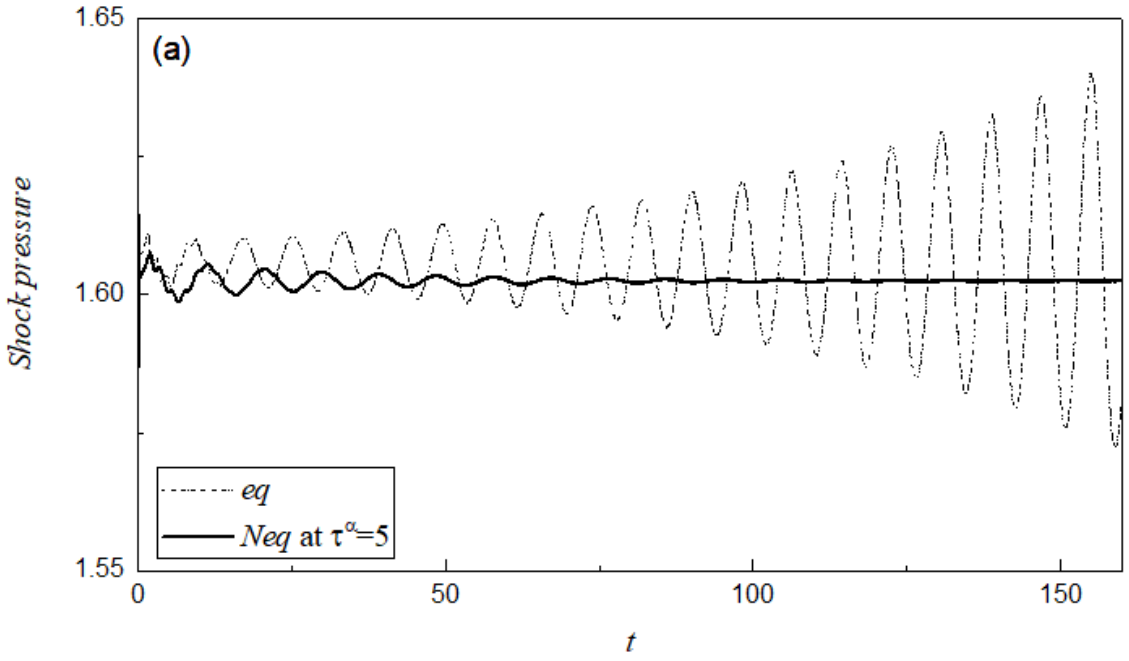

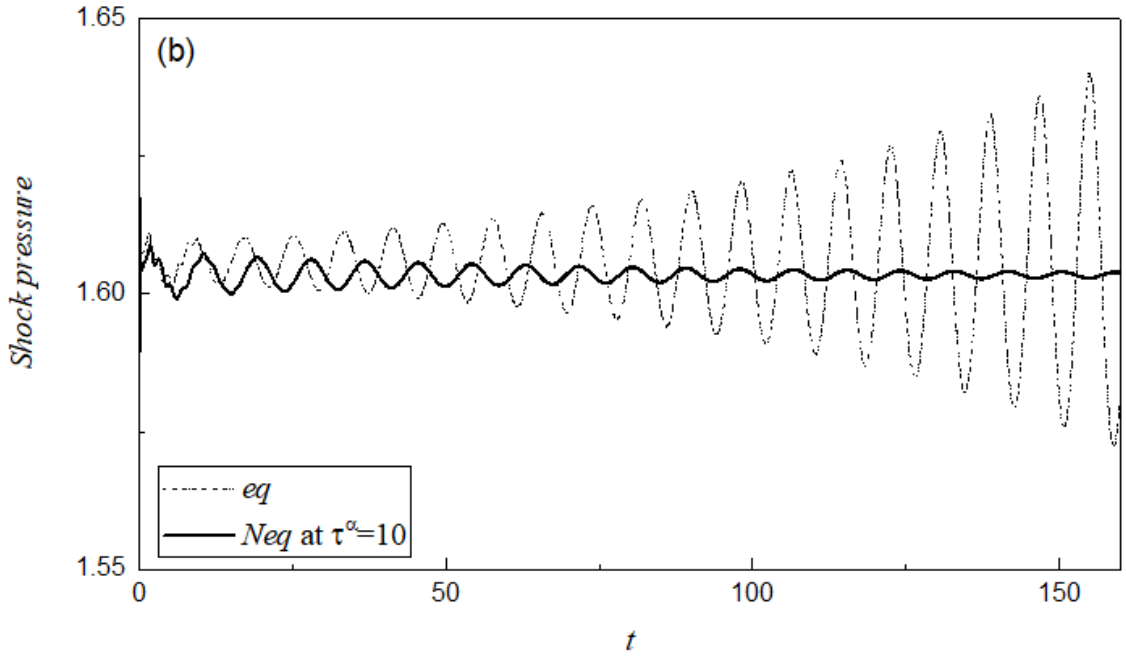
(b)
1.65
1.60
1.55
Shock pressure
0
50
100
150
t
eq
Neq at τ^α=10

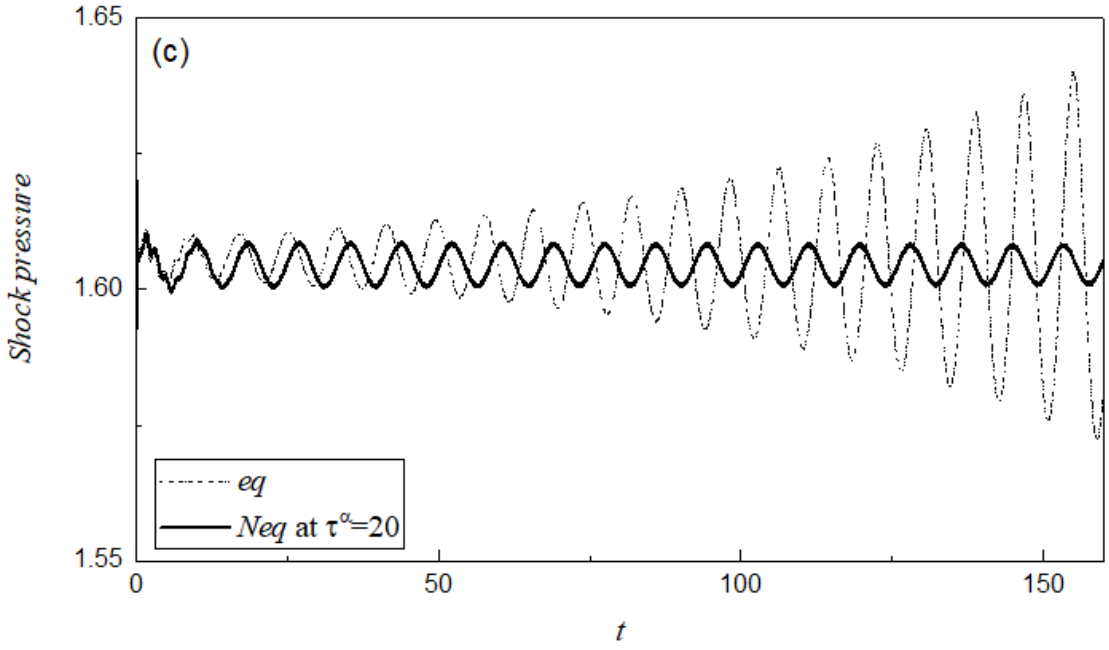
(c)
1.65
1.60
1.55
Shock pressure
0
50
100
150
t
eq
Neq at τ^α=20

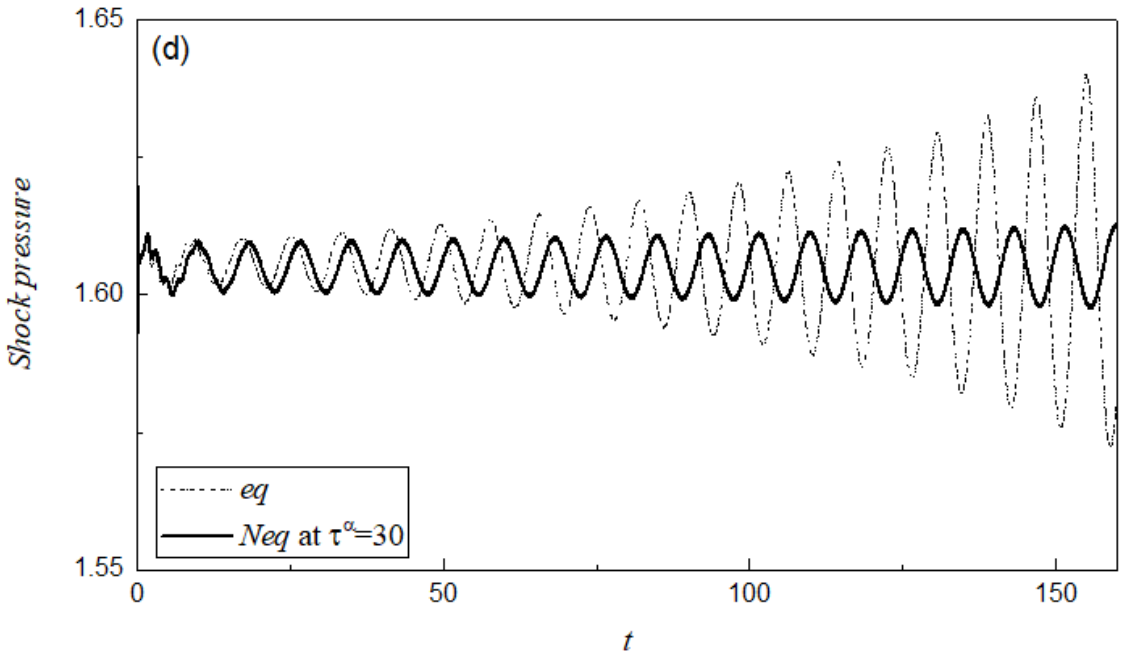

Fig. 4. Shock pressure history at $f = 1.6$ with vibrational nonequilibrium (*Neq*) case of a) $\tau^{\alpha} = 5$ (period = 9.32) b) $\tau^{\alpha} = 10$ (period = 8.74) c) $\tau^{\alpha} = 20$ (period = 8.43) and d) $\tau^{\alpha} = 30$ (period = 8.33) taking equilibrium case (*eq*) (period = 8.09) as reference. Other fixed parameters are $Q = 50$, $\gamma = 1.2$, $\vartheta = 20$ and $E_a = 50$

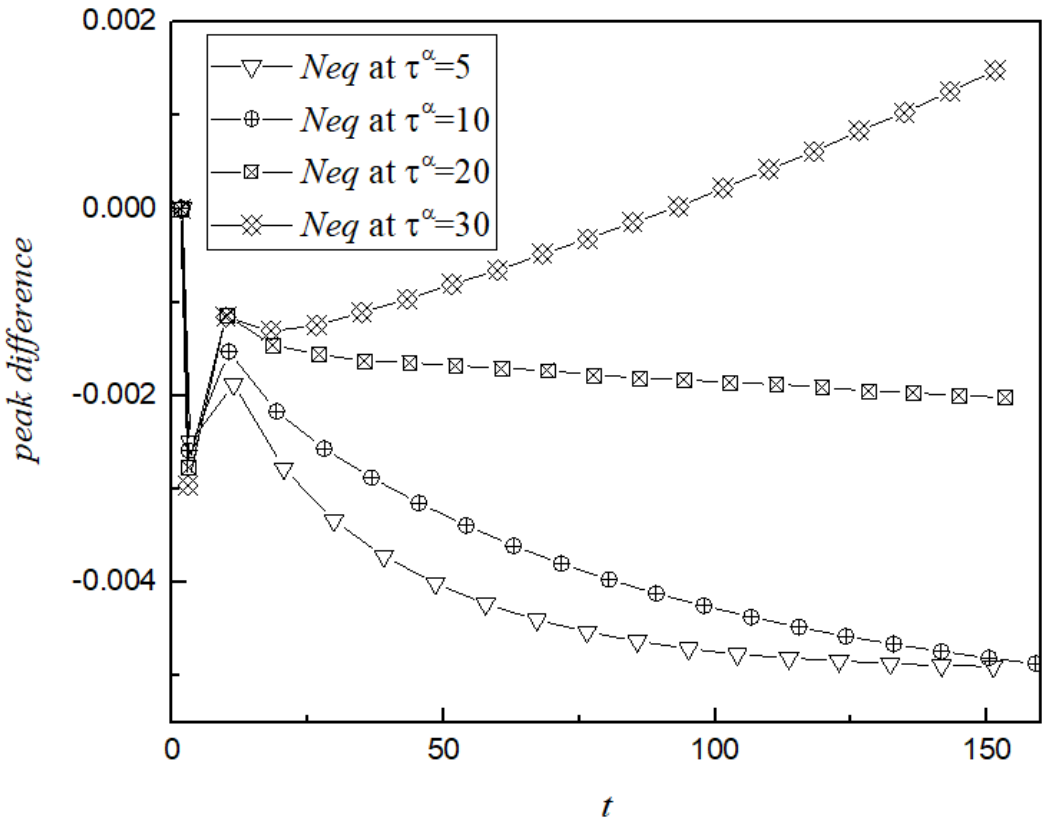

Fig. 5. The variations in the peak pressure difference with time for different vibrational nonequilibrium (*Neq*) cases in Fig. 4 at $\tau^{\alpha} = 5, 10, 20$ and 30.

4.4 Shock pressure history of detonation at thermal equilibrium state with different ϑ

In the above discussion, the characteristic vibrational temperature ϑ relevant to the vibrational energy content inside the system is fixed for demonstration. The change of ϑ in the system may possibly shift the stability limit to a large extent. Therefore, the effect of different ϑ (from 10 to 30) on the stability limit is presented in this section, while the other parameters are fixed, analogous to the neutral stable case of equilibrium state with vibrational energy included (i.e., $E_a = 26.47$, $Q = 50$, $\gamma = 1.2$ and $f = 1.0$ presented in section 4.1).

Figure 6 shows the peak difference analysis for the tested range of ϑ. Note that a startup error appears again at the beginning of the profile. As expected, the detonation is neutrally stable at $\vartheta = 20$, and the instability becomes severe at the high ϑ case. In other words, the stability limit of E_a should be much smaller for these cases, i.e., $E_a < 26.47$. Notably, if ϑ is large, denoting a small vibrational energy content considered in the system, the limit would be shifted to the thermal equilibrium case where the vibrational relaxation is neglectable, i.e., $E_a = 25.27$. On the other hand, for the cases of $\vartheta < 20$, the peak pressure difference history decays at first (see $\vartheta = 15$ in Fig. 6), and then the instability is developed again when ϑ further decreases (see $\vartheta = 10$). A local maximum of stability limit is foreseen at around $\vartheta = 15$, and the stability limit shifts to a lower value of E_a again if ϑ keeps decreasing. With a search of neutral stability limit similar to the work done in section 4.1, it is found that the limit with $\vartheta = 15$ is at $E_a = 26.62$ while $Q = 50$, $\gamma = 1.2$ and $f = 1.0$ are fixed. Hence, the range of stability limit of E_a evaluated by considering the vibrational relaxation in CJ detonation would be within a range from $E_a = 25.27$ to $E_a = 26.62$, depending on the choice of ϑ. Similarly, the range of stability limit of f in an overdriven detonation while $E_a = 50$, $Q = 50$, $\gamma = 1.2$ are fixed would be within a range from $f = 1.624$ (i.e., evaluated at the case of $\vartheta = 15$ following the approach in section 4.1) to $f = 1.731$ (i.e., the equilibrium case while vibrational

relaxation is neglectable). How sensitive these stability limits actually are to changes in the fixed vibrational temperature variable for the cases of mildly unstable detonation stated in section 4.2 and 4.3 are verified based on the above conclusions. It is worth noting that the choice of ϑ in the modelling should base on the actual species-interaction in the simulation which varies case by case.

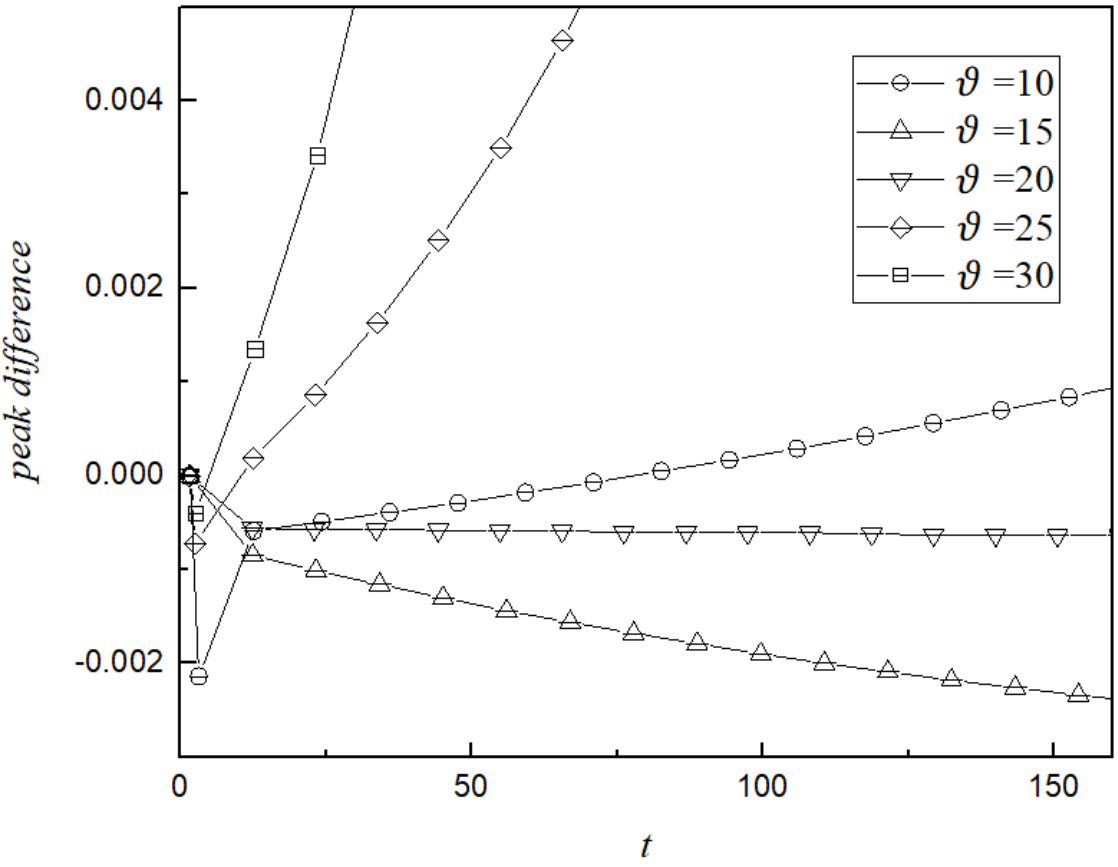

Fig. 6. The variations in the peak pressure difference with time at $\vartheta = 10, 15, 20, 25$ and 30. Other fixed parameters are $Q = 50$, $\gamma = 1.2$, $f = 1.0$ and $E_a = 26.47$.

5. Conclusion

In this paper, one-dimensional CE/SE numerical simulations of a propagating detonation are performed by considering the vibrational relaxation mechanism coupled with simplified chemical kinetics using Park's two-temperature model. A ratio of the chemical reaction time scale to the vibrational relaxation time scale, τ^{α}, is introduced to describe the different degrees of vibrational nonequilibrium. The steady-state ZND profile is extended to include the vibrational energy term and serves as an initial condition

in the simulations. The stability boundary of the activation energy for the corresponding detonation cases with $Q = 50$, $\gamma = 1.2$ and $\vartheta = 20$ is determined to be $E_a = 26.47$ under thermal equilibrium.

To elucidate whether the propagating detonation would be stabilized or destabilized under thermal nonequilibrium, mildly unstable cases for a CJ detonation and an overdriven detonation are simulated with different values of τ^α. In a CJ detonation with $E_a = 27$, which is unstable at an equilibrium state, the shock pressure histories of the selected cases show that a smaller amplitude and longer period of oscillation are observed as τ^α decreases. The critical τ^α at which the vibrational nonequilibrium effect becomes significant is 7.2. It is concluded that detonation stability is sensitive to the vibrational relaxation process, and stability behaviour is expected to be the same with the equilibrium case when τ^α is large, where the vibrational relaxation becomes insignificant in the chemical reaction. In other words, the high activation energy for detonation stability is expected at a vibrational nonequilibrium condition. A shift of the neutral stability limit results as τ^α varies.

In the second case with the overdriven factor f fixed at 1.6, which is mildly unstable under the equilibrium state, the result again shows that the pulsation is stabilized at a small τ^α value, reflected by a small amplitude and a long period of oscillation in the shock pressure history. The critical τ^α below which the pulsation shows a decay with time is approximately 21. Since both the change in f and τ^α are equally crucial in stabilizing the detonation, the decrease in τ^α attributed to the significance of the vibration-chemistry coupling effect reduces the stability limit of f for the selected case.

The effect of ϑ on the shift of stability limit is addressed in the end. Based on the analysis of the case with $E_a = 26.47$ which is neutral stable at $\vartheta = 20$, it is suggested that the maximum shift of stability limit would be at around $\vartheta = 15$. However, the choice of ϑ in the model should follow the actual species-interaction in the realistic simulations.

In this numerical research, the effect of the vibration-chemistry coupling effect is manifested in terms of the time ratio τ^α. The results suggest that the detonation propagation is stabilized under the effect of vibrational nonequilibrium, and hence, a shift of the neutral stability limit is predicted. The actual stability limit for each studied case requires further study, and linear stability analysis will also be considered. Furthermore, for simplicity, a one-step chemical model is utilized in this report to describe the reaction process. However, an induction zone should also be considered if the chain-branching

kinetics is included. Therefore, the coupling effect among the three timescales – induction time scale, chemical reaction time scale and vibrational relaxation time scale, is worth investigated in the future. From the above analysis, the significance of considering vibrational nonequilibrium in detonation stability for propulsion device design is addressed regardless.

Acknowledgement

The authors would like to thank the Hong Kong Research Grants Council (no. 152065/19E) for financial support.

References

[1] B. Zhang, H. Liu, B. Yan, Velocity behavior downstream of perforated plates with large blockage ratio for unstable and stable detonations, Aerospace Science and Technology, 86 (2019) 236-243.
[2] Y. Fang, Z. Hu, H. Teng, Z. Jiang, H.D. Ng, Numerical study of inflow equivalence ratio inhomogeneity on oblique detonation formation in hydrogen–air mixtures, Aerospace Science and Technology, 71 (2017) 256-263.
[3] Q. Meng, N. Zhao, H. Zheng, J. Yang, Z. Li, F. Deng, A numerical study of rotating detonation wave with different numbers of fuel holes, Aerospace Science and Technology, 93 (2019) 105301.
[4] D.S. Stewart, A.R. Kasimov, State of Detonation Stability Theory and Its Application to Propulsion, Journal of Propulsion and Power, 22 (2006) 1230-1244.
[5] Y.B. Zeldovich, On the theory of the propagation of detonation in gaseous systems, (1940).
[6] J. Von Neumann, Theory of detonation waves, O.S.R.D. Rept., 1942, pp. 549.
[7] W. Döring, Über den Detonationsvorgang in Gasen [On detonation processes in gases], Annalen der Physik, 43 (1943) 421-436.
[8] W. Fickett, W.C. Davis, Detonation, University of California Press1979.
[9] G.J. Sharpe, S.A.E.G. Falle, Numerical simulations of pulsating detonations: I. Nonlinear stability of steady detonations, Combustion Theory and Modelling, 4 (2000) 557-574.
[10] G.J. Sharpe, Numerical simulations of pulsating detonations: II. Piston initiated detonations, Combustion Theory and Modelling, 5 (2001) 623-638.
[11] M. Short, G.J. Sharpe, Pulsating instability of detonations with a two-step chain-branching reaction model: theory and numerics, Combustion Theory and Modelling, 7 (2003) 401-416.
[12] J.J. Erpenbeck, Stability of Steady-State Equilibrium Detonations, Physics of Fluids, 5 (1962) 604-614.
[13] J.J. Erpenbeck, Structure and stability of the square-wave detonation, Symposium (International) on Combustion, 9 (1963) 442-453.
[14] J.J. Erpenbeck, Stability of Idealized One-Reaction Detonations, Physics of Fluids, 7 (1964) 684.
[15] H. Lee, D.S. Stewart, Calculation of linear detonation instability: one-dimensional instability of plane detonation, Journal of Fluid Mechanics, 216 (1990) 103-132.

[16] H.D. Ng, M.I. Radulescu, A.J. Higgins, N. Nikiforakis, J.H.S. Lee, Numerical investigation of the instability for one-dimensional Chapman–Jouguet detonations with chain-branching kinetics, Combustion Theory and Modelling, 9 (2005) 385-401.
[17] S.D. Watt, G.J. Sharpe, Linear and nonlinear dynamics of cylindrically and spherically expanding detonation waves, Journal of Fluid Mechanics, 522 (2005) 329-356.
[18] G.J. Sharpe, S.A.E.G. Falle, One-dimensional nonlinear stability of pathological detonations, Journal of Fluid Mechanics, 414 (2000) 339-366.
[19] G.J. Sharpe, Linear stability of pathological detonations, Journal of Fluid Mechanics, 401 (1999) 311-338.
[20] H. Koo, V. Raman, P.L. Varghese, Direct numerical simulation of supersonic combustion with thermal nonequilibrium, Proceedings of the Combustion Institute, 35 (2015) 2145-2153.
[21] R. Fiévet, S. Voelkel, H. Koo, V. Raman, P.L. Varghese, Effect of thermal nonequilibrium on ignition in scramjet combustors, Proceedings of the Combustion Institute, 36 (2017) 2901-2910.
[22] S. Voelkel, V. Raman, P.L. Varghese, Effect of thermal nonequilibrium on reactions in hydrogen combustion, Shock Waves, 26 (2016) 539-549.
[23] L. Shi, H. Shen, P. Zhang, D. Zhang, C. Wen, Assessment of Vibrational Non-Equilibrium Effect on Detonation Cell Size, Combustion Science and Technology, 189 (2016) 841-853.
[24] K.C.K. Uy, L. Shi, C.Y. Wen, Chemical reaction mechanism related vibrational nonequilibrium effect on the Zel'dovich−von Neumann−Döring (ZND) detonation model, Combustion and Flame, 196 (2018) 174-181.
[25] B. Taylor, D. Kessler, E. Oran, Estimates of Vibrational Nonequilibrium Time Scales in Hydrogen-Air Detonation Waves, 24th International Colloquium on the Dynamics of Explosive and Reactive SystemsTaipei, Taiwan, 2013.
[26] W.G. Vincenti, C.H. Kruger, Introduction to physical gas dynamics, 1965.
[27] B. Taylor, D. Kessler, V. Gamezo, E. Oran, Numerical simulations of hydrogen detonations with detailed chemical kinetics, Proceedings of the combustion Institute, 34 (2013) 2009-2016.
[28] K.C.K. Uy, L. Shi, C.Y. Wen, Prediction of half reaction length for H2O2Ar detonation with an extended vibrational nonequilibrium Zel'dovich −von Neumann −Döring (ZND) model, International Journal of Hydrogen Energy, 44 (2019) 7667-7674.
[29] H. Ng, A. Higgins, C. Kiyanda, M. Radulescu, J. Lee, K. Bates, N. Nikiforakis, Nonlinear dynamics and chaos analysis of one-dimensional pulsating detonations, Combustion Theory and Modelling, 9 (2005) 159-170.
[30] R.C. Millikan, D.R. White, Systematics of vibrational relaxation, The Journal of chemical physics, 39 (1963) 3209-3213.
[31] S.-C. Chang, The method of space-time conservation element and solution element—a new approach for solving the Navier-Stokes and Euler equations, Journal of Computational Physics, 119 (1995) 295-324.
[32] C.Y. Wen, H. Saldivar Massimi, H. Shen, Extension of CE/SE method to non-equilibrium dissociating flows, Journal of Computational Physics, 356 (2018) 240-260.
[33] H. Shen, C.-Y. Wen, M. Parsani, C.-W. Shu, Maximum-principle-satisfying space-time conservation element and solution element scheme applied to compressible multifluids, Journal of Computational Physics, 330 (2017) 668-692.

[34] H. Shen, C.-Y. Wen, A characteristic space–time conservation element and solution element method for conservation laws II. Multidimensional extension, Journal of Computational Physics, 305 (2016) 775-792.
[35] H. Shen, C.-Y. Wen, D.-L. Zhang, A characteristic space–time conservation element and solution element method for conservation laws, Journal of Computational Physics, 288 (2015) 101-118.
[36] H. Shen, C.-Y. Wen, K. Liu, D. Zhang, Robust high-order space–time conservative schemes for solving conservation laws on hybrid meshes, Journal of Computational Physics, 281 (2015) 375-402.
[37] H. Shen, M. Parsani, The role of multidimensional instabilities in direct initiation of gaseous detonations in free space, Journal of Fluid Mechanics, 813 (2017).
[38] M. Short, D.S. Stewart, Cellular detonation stability. Part 1. A normal-mode linear analysis, Journal of Fluid Mechanics, 368 (1998) 229-262.
[39] J.H. Lee, The detonation phenomenon, Cambridge University Press Cambridge2008.
[40] L. He, J.H. Lee, The dynamical limit of one-dimensional detonations, Physics of Fluids, 7 (1995) 1151-1158.